Heat transfer and flow field in a circular twisted channel

Suvanjan Bhattacharyya[1,*], *Himadri* Chattopadhyay[2], *Arnab* Banerjee[3], and *Ali Cemal* Benim[4]

[1]Deparement of Mechanical and Aeronautical Engineering, University of Pretoria, South Africa
[2]Mechanical Engineering Department, Jadavpur University, Kolkata, West Bengal, India
[2]Mechanical Engineering Department, MCKV Institute of Engineering, Liluah, Howrah, West Bengal, India
[4]Center of Flow Simulation (CFS), Dept. Mechanical and Process Engineering, Düsseldorf University of Applied Sciences, Germany

Abstract. In the present paper, along with experimental study, computational fluid dynamics analysis is performed, using the transition SST model which can predict the change of flow regime from laminar through transition to turbulent. The differential governing equations are discretized by the finite volume method. The investigations are conducted for Reynolds numbers ranging from 100 to 50,000 covering laminar, transitional and turbulent regimes, and for three length and three pitch ratios. The predictions are observed to show a good agreement with the measurements and published correlations of other authors. The analysis indicates that the large length ratio and small pitch ratio yields a higher heat transfer rate with relatively low performance penalty. The transition from laminar to turbulent regime is observed between Reynolds numbers of 2,500 to 3,500 for all cases. For almost all investigated cases the performance factors are greater than unity.

1 Introduction

Heat exchanger is a device facilitating heat transfer between two or more fluids [1]. It is used in a vast number of industrial applications, such as thermal power plants, chemical processing plants, air conditioning equipment, refrigerators, radiator for space vehicles as well as automobiles, extending up to micro-scale applications [2,3]. Obviously, for improving the efficiency of energy utilization, enhancement of heat transfer in such applications play an important role. To this goal, two techniques can generally be identified, namely, the active and passive techniques. Active techniques include surface vibration, fluid vibration etc. for increasing heat transfer [4]. In passive techniques, the applied methods usually involve a modification of the channel geometry to enhance heat transfer. A special category herein is the use of bluff bodies that increase heat transfer by vortex shedding [5,6]. Passive methods may also include basically different arrangements, such as impinging jet [7,8] instead of wall-parallel flow.

A further passive technique that attracted considerable attention is the insertion of structures such as twisted tapes that induce a swirling motion. Indeed, industrial heat transfer equipment are generally operated in turbulent/swirl flow conditions where their performance in terms of energy transfer rate is high, compared with laminar flow by virtue of the high degree of turbulence in turbulence/swirl flow. Heat transfer characteristics under transitional flow conditions in most of thermal problems are of considerable interest. Predicting transition of laminar regime to turbulent in heat transfer augmentation techniques will be highly useful to design any heat transfer equipment. There is constant thrive in the studies on transition from laminar to turbulent flow.

Many researchers performed surveys on passive enhancement method of this kind, which were very inspiring, such as channel with a cylinder roughness [9] and compound heat transfer enhancement of a convergent-divergent tube with a twisted tape [10].Swirling flow may increase the heat transfer through the boundary layer by interruption or thinning and also increase turbulence intensity [11]. Tube with wire coil inserts [12] can generate vortex and also can develop secondary flow. Tube insert technology – i.e., insertion of tape inside a channel - was used in some previous work. Bhattacharyya et al. [13,14] and Saha et al. [15] studied experimentally center-clearing twisted tapes with artificial rib roughness and achieved considerable improvement. Meng et al. [16] performed experiments on elliptical tube type swirl generator. Some earlier research [17,18] showed that vortex geometry may effect heat transfer and be utilized to design heat exchangers. Chen et al. [19] studied experimentally heat transfer augmentation techniques of a dimpled tube. Vicente et al. [20] reported on thermohydraulic performance of a helically dimpled tubes for laminar and transition flow. Mengna et al. [21] studied on compound heat transfer enhancement of a converging–diverging tube with swirl generator inserts. Sivashanmugam et al. [22] reported on experiments on thermohydraulic characteristics of laminar stream in circular channel fitted with screw type tape. Additional information on similar vortex originator might be acquired from [23–27].

In the present paper, a numerical and experimental study of forced convection in circular twisted channel is

* Corresponding author: suvanjanmechanical@gmail.com

presented. Air is used as working medium. At the prevailing relatively small/moderate temperature differentials, constant material properties are assumed A sketch of the device is presented in Figure 1, where the circular twisted enhancer can be recognized.

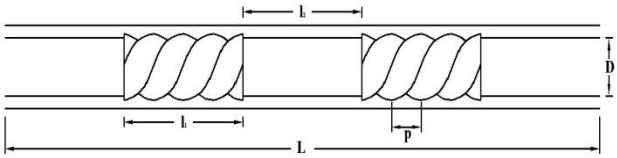

Fig. 1. Sketch of geometry.

2 Experimental rig

Figure 2 demonstrates the schematic figure and original look of the experimental setup. Labeled portions show the significant parts of the test rig in which experiment is prosecuted. Air is considered as the working medium while carrying out the experiment. The experiment is conducted in a non-air conditioned laboratory and usually the temperature in the room is varied between 27°C - 33°C.

The atmospheric air was sucked by a 7.0 kW blower. This air is then crossed throughout a PVC (Polyvinyl chloride) made pipe and finally comes to a rotameter. The rotameter is utilized to assess the mass flow rate of the employed fluid (Pr = 0.707). With higher blower speed the mass flow rate fluctuation decreases. A bypass valve is installed in between the blower and the rotameter. The foremost intention of this bypass valve is to pass the excess air through this valve and maintain a low mass flow rate. The rotameter can assess flow rate varying in between 120 to 520 LPH. An error of 0.0442% is present in the rotameter. U-tube manometer is utilized to assess the pressure drop along the test section. Three circular twisted channels of different length ratios (H = l/L = 0.2, 0.25 and 0.30), and three different pitch ratios (S = p/d = 0.22, 0.36, and 0.45) were used for evaluation.

3 Test section

For validation purpose the experiment is executed in a smooth tube and then the twisted parts are installed which are used to enrich the heat transfer rate. A circular corrugated tube having 22 mm inside diameter and length of 2.0 m is used for the experiment purpose. The channel as depicted in Figure 1 is made up of brass. In order to assess the pressure drop throughout the experiment two pressure taps are placed in the experimental setup. The two pressure taps are placed at inlet and outlet of the test section. Net distance between the two pressure taps is 2.10 m. The pressure taps are placed in such a way such that they can only assess the pressure values of the fully developed flow. The pressure drop is measured using a differential U-tube manometer ranging from 0 -150 mm Hg. The differential manometer is calibrated to ensure no error.

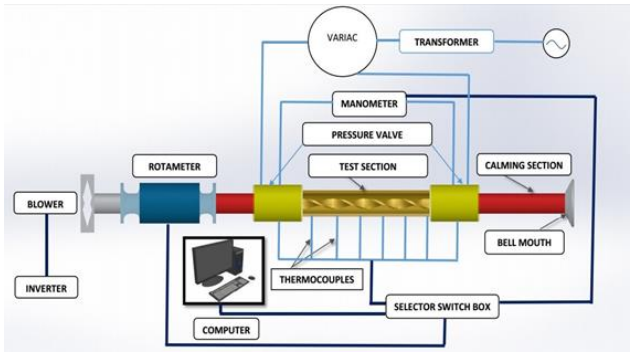

(a)

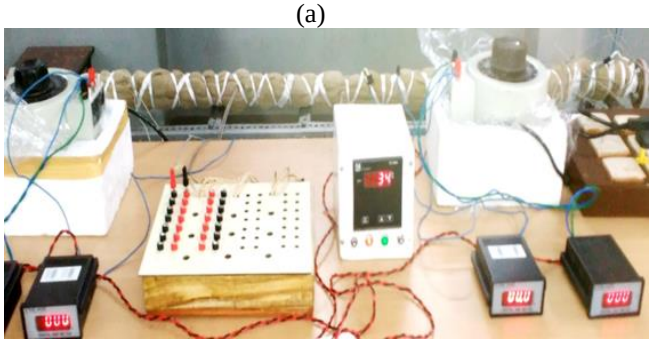

(b)

Fig. 2. Schematic diagram (a) and photographic view (b) of experimental setup.

A total of 28 thermocouples were fitted on the tube outside wall by brazing. The thermocouples are installed at 7 locations. The positions of thermocouples were 10 cm, 60 cm, 1.00 m, 1.35 m, 1.6 m, 1.75 m and 1.90 m over the wall of corrugated tube. Each position contains 4 thermocouples.

The test section was electrically heated up by nichrome heater wire providing uniform wall heat flux boundary condition. Porcelain bead types of insulation were used on nichrome heater wire, so no direct interaction of the nichrome heater wire with the tube wall. A 1.5 KW variac is used in which the variations of voltage and current are 10.0 – 30.0 V and 1.0 – 3.0 A respectively. There is an error of 0.072% in the current and voltage compared to the nominal value. In order to shrink the heat loss the brass corrugated tube is insulated using glass-wool having thermal conductivity 0.0037 W/mK that are tightly insulated by fabricated ropes. The total insulation thickness is 140 mm, and approximately 99% of the heat loss is prevented using such insulations.

A data accumulating system is used for recording all the measurements. The mass flow rate, inlet, outlet and bulk temperatures, differential pressure readings are taken and recorded in the data accumulating system. The output data from the data accumulating system is provided as an input into the personal computer which helps in data reduction.

4 Experimental procedure

The investigational setup is turned on and the voltage is setup at 20V to obtain the required heat flux. The setup is allowed to avail steady state by providing a time

allowance of approximately 1 hour and 45 minutes. For most of the experiments the upmost mass flow rate is maintained at 12 kg/s. When the standard deviation of the temperature and mass flow rate are less than 0.03°C and 0.011 kg/s respectively then it is assumed that steady state is attained. As soon as steady state is attained, the data accumulated system receives a set of 110 readings of all the temperatures, pressures and mass flow rates. First the experiment is conducted in the plain channel. After that the circular twisted channel was placed in place of plain channel. The experiment is conducted using three circular twisted channels of different length ratios (H = l/L = 0.2, 0.25 and 0.30), and three different pitch ratios (S = p/d = 0.22, 0.36, and 0.45). The experiment is conducted by the variation of mass flow rate for both plain channel and twisted channel. A total of 40 experiments are executed for plain channel and 75 experiments for twisted channel. Uncertainties of some major experimental variables are given in Table 1. The uncertainty in Reynolds number, friction factor and Nusselt number were estimated as $\pm$ 4.17 %, $\pm$ 6.66 % and $\pm$ 7.42 %, respectively following the procedure of Bhattacharyya and Saha [11,24].

5 Modelling

In the current numerical study, three-dimensional convective heat transfer (HT) augmentation of air through circular twisted channel as shown in Figure 1 is simulated. For modelling purposes, an unstructured grid with non-uniform grid density distribution was created, in order to observe the flow and heat transfer more accurately. The regions in the channel close to the channel wall are meshed into smaller control volumes in order to achieve a more precise prediction. Different grid sizes were tested as part of grid independence study. As result, a grid with 777,235 cells are selected as the numerical grid. The surface grid is shown in Figure 3.

In the present investigation, circular twisted channels of four different length ratios (H = l/L = 0.2, 0.25 and 0.30), and three different pitch ratios (S = p/d = 0.22, 0.36, and 0.45) are investigated. Fluid enters the channel at an inlet temperature (T_i) of 300 K. At the wall, a uniform wall temperature (T_w) boundary condition is employed with T_w=500 K, along with no slip. The range of Reynolds number considered is from 100 to 50,000. At the inlet, a uniform velocity profile is used with a turbulent intensity of 5%, even in the laminar regime following Abraham et al [28].

The governing equations are discretized on a non-uniform unstructured grid using finite volume method within the framework of the general purpose CFD code Ansys Fluent [29]. Buoyancy effects as well as radiation [30] are neglected. The SST model of turbulence [29] was successfully used in a wide spectrum of applications [28,31]. The transitional version of the SST model [29] is used as the turbulence model. Kadiyala et al. [32] used this model for studying the effect of jets on moving surface, Oclon et al. for predicting fouling in a compact heat exchanger [33] and Bhattacharyya et al. [34] for enhancement purposes. The velocities and pressures

Table 1. Experimental uncertainties of major parameters.

Name of variables	Errors
Flow velocity	0.18%
Voltage on the heater	0.15%
Electrical resistance	0.33%
Heat transfer coefficient	1.19%
Current on the heater	0.23%
Ambient temperature	0.10%
Electrical power on the heater	0.17%
Average temperature	0.60%

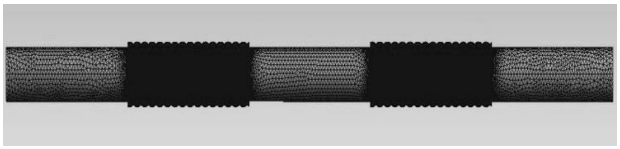

Fig. 3. Surface grid (detail).

were predicted using the SIMPLE scheme. For convective terms, a second order upwind scheme [29] is used. The discretized equations are then solved iteratively using in double precision. The convergence criteria for continuity, momentum and energy are set at 10^{-4}, 10^{-5}, and 10^{-7} respectively. The convergence criterion for the other four turbulence quantities was also fixed at 10^{-4} [29]. The Reynolds number of air flow in the channel is calculated from, where U, D_h, ν denote the bulk velocity, hydraulic diameter and kinematic viscosity, respectively

$$\mathrm{Re} = \mathrm{U}\mathrm{D}_\mathrm{h} / \nu \qquad (1)$$

The heat transfer coefficient (h) is, then, obtained from where q_w, T_w, T_b denote the wall heat flux, wall temperature and bulk fluid temperature, respectively.

$$\mathrm{h} = \mathrm{q}_\mathrm{w} /(\mathrm{T}_\mathrm{w} - \mathrm{T}_\mathrm{b}) \qquad (2)$$

The convective heat transfer coefficient is then used to obtain Nusselt number (Nu) as, where k denotes the thermal conductivity

$$\mathrm{Nu} = \mathrm{h}\mathrm{D}_\mathrm{h} / \mathrm{k} \qquad (3)$$

The friction factor is determined from the measured values of pressure drop (Δp), across the test section length using the following relation (L is tube length).

$$\mathrm{f} = 2\mathrm{D}_\mathrm{h}\Delta\mathrm{p} / \rho\mathrm{L}\mathrm{U}^2 \qquad (4)$$

To evaluate the effect of heat transfer enhancement under given pumping power, the performance evaluation criteria η (Bhattacharyya et al. [35]) is determined as

$$\eta = \mathrm{Nu}\,\mathrm{f}_0^{0.33} / \mathrm{Nu}_0\,\mathrm{f}^{0.33} \qquad (5)$$

where the subscript 0 denotes the plain tube.

The field synergy principle has a special application. To reveal the variation of the included angle between velocity and temperature Guo et al. [36] employed

$$\beta_\mathrm{m} = \cos^{-1}\left(\int|\vec{\mathrm{u}}||\vec{\nabla}\mathrm{T}|\cos\beta\mathrm{dV} / \int|\vec{\mathrm{u}}||\vec{\nabla}\mathrm{T}|\mathrm{dV}\right) \qquad (6)$$

5 Results

In order to inspect the heat transfer augmentation of the horizontal heated twisted channel, the Nusselt numbers of the channel with twisted geometry were evaluated as shown in Figure 4 for selected cases. It is observed that the Nusselt number raises with a raise in the Reynolds number (Re). This is indeed expected. Based on the Nusselt numbers, it is evident that the channel with twisted geometry have higher convective heat transfer (HT) compared that of the plain channel [1]. Interruption of the fluid flow (starting from the inlet of the experimental rig) owing to the occurrence of the twist leads to secondary flows and enhances fluid mixing [37]. It is also clear from Figure 4 that the Nusselt numbers are higher for small pitch ratio (S = p/d). This is likely because a small pitch ratio promotes flow recirculation and separation, which underside of the wake swirls to the upper side, interacting with the thermal boundary layer. As the fluid passes, the twisted portion enhances mixing between the core and surface. The Nu rises by 51% compared to the plain channel [1].

The friction penalty was used to assess the characteristics of fluid flow in this study. Figure 5 shows the variations of the friction factor (f) with the Reynolds number. It can be viewed that the 'f' reduces with a raise in Re. The 'f' are higher for the twisted channel evaluated with those for the plain channel, which is likely due to the increase in the contact surface area and reduced free flow, which increases the flow velocity. It is apparent that the friction factors are higher for the twisted channel small pitch ratio (S = p/d) evaluated against the other pitch ratios and plain channel [1]. The fluid is transported toward the channel walls due to the generation of secondary flow, which deforms the profiles of axial velocity along the length of the channel.

Turbulent Intensity at the exit of the channel is shown in Figure 6. Turbulent dies out for low Reynolds number (Re = 100) and increases with increasing Reynolds number. At the entry of the tube the TI is given 5% [38]. From the Figure 6, one can see that the highest level of turbulent intensity is about 14%-15% at Reynolds number of 40,000 - 50,000.

Figure 7 shows the variations of the thermal performance with the Re of the twisted channel. It can be distinguished that the thermal performance is more than unity for most of the time in varied Re. At higher Re (Re = 35000 – 50000) for the case of H = 0.2 and S = 0.45, the thermal performance decreases to a value less than 1.0. $\eta \geq 1.0$ indicates that the heat transfer for the channel with twisted geometry is higher than that for the plain one for the same pumping power. Figure 7 also shows that the thermal performance of the channel with twisted geometry increases with an increase of length ratio (H = l/L) and decrease in pitch ratio (S = p/d). The highest thermal performance is obtained for channel with H = 0.3 and S = 0.22. The lowest thermal performance is obtained for the channel with H = 0.2 and S = 0.45.

The synergy principle analysis [36] helps to realize the actual enhancement caused due to the presence of the twisted channel. Major part of the flow domain is redistricted to synergy angle close to 90^0. This is the reason the average synergy angle for each case is lies in the range of 87^0 to 90^0 as seen in Figure 8. The general nature of the synergy angle is to increase with increase in Reynolds's number. It is also evident that as the flow reaches turbulence there is a clear increase in the synergy angle. This could be used to explain why we see such a dramatic drop in the efficiency at the turbulent region. Again, it is visible that the increase in length ratio with small pitch ratio decreases the synergy sufficiently to provide good heat transfer enhancement which is also supported by the evidence in the efficiency.

5 Conclusions

In this work, the heat transfer and fluid flow characteristics of turbulent flow through a heat exchanger mounted with circular twisted channel were investigated experimentally and numerically. It is observed the twisted geometry enhances heat transfer considerably. Heat transfer also increases with an increase of length ratio and decrease in pitch ratio. The

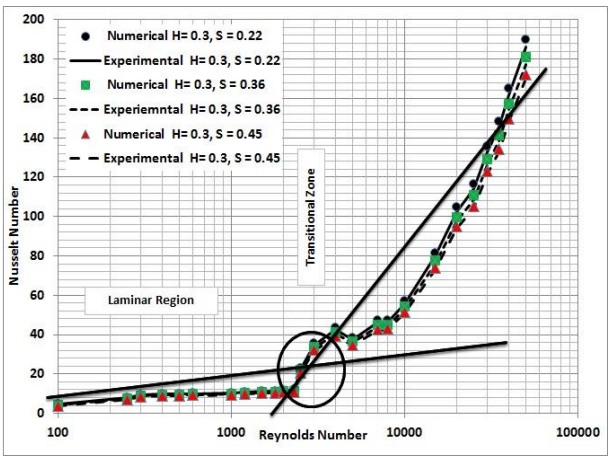

Fig. 4. Nusselt number as function of Reynolds number, (a) at constant value of length ratio (H = 0.3) with different pitch ratio (S = 0.22, 0.36, 0.45).

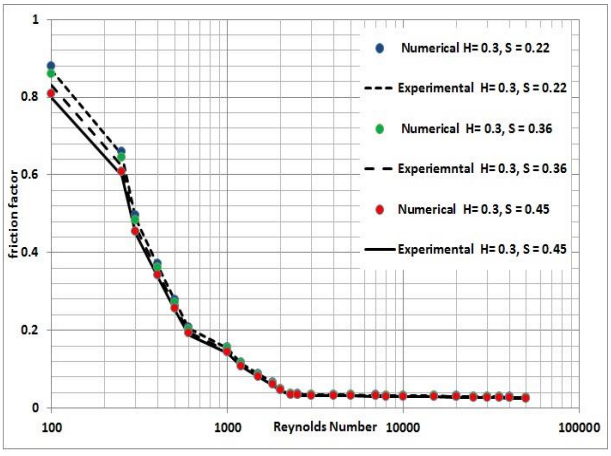

Fig. 5. Friction factor as function of Reynolds number, (a) at constant value of length ratio (H = 0.3) with different pitch ratio (S = 0.22, 0.36, 0.45).

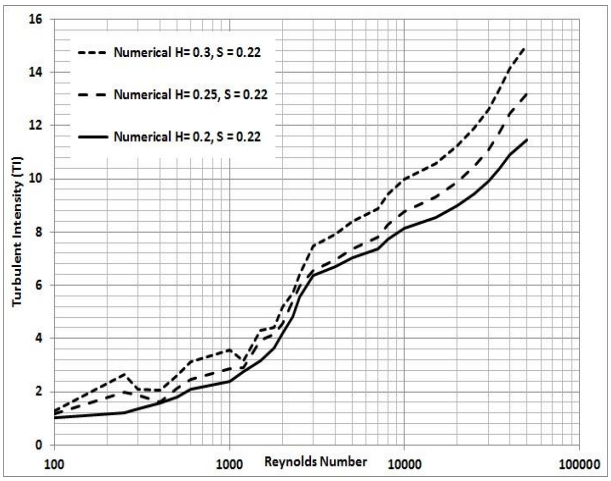

Fig. 6. Variation of turbulent intensity (TI) with Re.

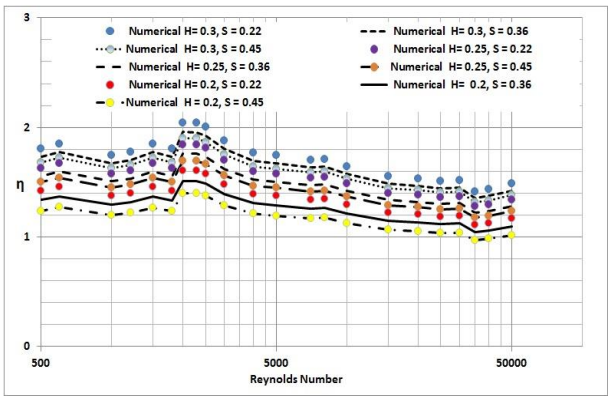

Fig. 7. Thermal enhancement factor.

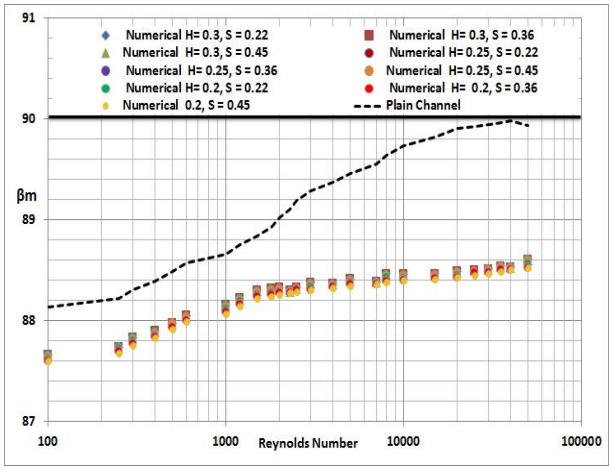

Fig. 8. Variation of average synergy angle with Reynolds number for different length and pitch ratio.

twisted geometry with the large length ratio and small pitch ratio leads to the highest heat transfer augmentation, where the Nu is higher by 51% compared with those for the plain channel. The friction factor decreases as the Re increases, but increases increasing length ratio and decreasing pitch ratio. In spite of the high friction penalty, H=0.3 and S=0.22 yields the maximum thermal performance, with a value of 2.08.

References

1. K.R. Shah, D.P. Sekulic, *Fundamentals of Heat Exchanger Design* (Wiley, Chichester, UK, 2003)
2. A.M. Maqableh, A.F. Khadrawi, M.A. Al-Nimr, S. A. Ammourah, A.C. Benim, Progress in Computational Fluid Dynamics, **11,** 5, pp.318-328 (2011)
3. D.G. Ebling, A. Krumm, B. Pfeiffelmann, J. Gottschald, J. Bruchmann, A.C. Benim, M. Adam, R. Labs, R.R. Herbertz, A. Stunz, Journal of Electric Materials, **45,** 7, pp.3433-3439 (2016)
4. A.C. Benim, M. Cagan, D. Gunes, International Journal of Thermal Sciences, **43,** 8, pp.725-732 (2004)
5. A.C. Benim, H. Chattopadhyay, A. Nahavandi, International Journal of Thermal Sciences, **50,** 10 pp.1973-1983 (2011)
6. I. Taymaz, E. Aslan, A.C. Benim, **19,** 2, pp. 537-547 (2015)
7. H. Chattopadhyay, A.C. Benim, Journal of Heat Transfer – Transactions of the ASME, **133,** 10, Article Number: 104502, 5 pages (2011)
8. A.C. Benim, K. Ozkan, M. Cagan, D. Gunes, International Journal of Numerical Methods for Heat & Fluid Flow, **17,** 3, pp.284-301 (2007)
9. N. Mahir, Z. Altaç, Heat Transfer Eng., **38,** 16, pp.1367 – 1381 (2016)
10. M. Hong, X. Deng, K. Huang, Z. Li, Chinese J. Chemical Eng., **15,** 6, pp.814-820 (2007)
11. A.C. Benim, M.P. Escudier, A. Nahavandi, A.K. Nickson, K.J. Syed, F. Joos, International Journal of Numerical Methods for Heat & Fluid Flow, **20,** 3, pp.348-370 (2010)
12. P.K. Rout, S.K. Saha, ASME J Heat Transfer, **135,** 2, Article Number: 021901 (2013)
13. S. Bhattacharyya, S. Saha, S.K. Saha, Exp. Thermal Fluid Science, **44**, pp.727-735 (2013)
14. S. Bhattacharyya, S.K. Saha, Experimental Thermal and Fluid Science, **42**, pp. 154-162 (2012)
15. S.K. Saha, S. Bhattacharyya, P.K. Pal, Exp. Therm.Fluid Sci., **41**, pp.121-129 (2012)
16. J.A. Meng, X.G. Liang, Z.J. Chen, Z.X. Li, Experimental Thermal and Fluid Science, **29,** pp.457-465 (2005)
17. S.K. Saha, ASME Journal Heat Transfer, **132,** 8, Article Number: 081701, 12 pages (2010)
18. A. Mwesigye, T. Bello-Ochende, J. P. Meyer, International Journal of Thermal Sciences, **99**, pp.238-257 (2016)
19. J. Chen, H. Müller-Steinhagen, G.G. Duffy, Applied Thermal Engineering, **21**, pp.535–547 (2011)
20. P.G. Vicente, A. Garcia, A. Viedma, International Journal of Heat and Mass Transfer, **45**, pp.5091–5105 (2002)
21. H. Mengna, D. Xianhe, H. Kuo, L. Zhiwu, Chinese Journal of Chemical Engineering, **15**, pp.814–820 (2007)

22. P. Sivashanmugam, S. Suresh, Applied Thermal Engineering, **26,** 16, pp.1990-1997 (2006)
23. G. Biswas, H. Chattopadhyay, A. Sinha, Heat Transfer Engineering, **33,** 4, pp.406-424 (2012)
24. P. Kumar, F. Topin, M. Miscevic, P. Lavieille, L. Tadrist, Numerical Heat and Mass Transfer in Porous Media, Advanced Structured Materials, **27**, pp.181–208 (2012)
25. B. Li, B. Feng, Y.L. He, W.Q. Tao, Appl. Thermal Eng., **26**, pp.2336-2344 (2006)
26. S.K. Saha, S. Bhattacharyya, G.L. Dayanidhi, Heat Trans. Research, **43,** 3, pp. 207-227 (2012)
27. S. Bhattacharyya, H. Chattopadhyay, S. Bandyopadhyay, International J. Heat and Technology, **34,** 3, pp. 401-406 (2016)
28. J.P. Abraham, E.M. Sparrow, J.C.K. Tong, Int. Journal of Heat and Mass Transfer, **52,** 3-4, pp. 557–563 (2009)
29. www.ansys.com
30. A.C. Benim, Computer Methods in Applied Mechanics and Engineering", **67,** 1, pp.1-14 (1988)
31. A. Assmann, A.C. Benim, F. Gül, P. Lux, P. Akhyari, U. Boeken, F. Joos, P. Feindt, A. Lichtenberg, Journal of Biomechanics, **45,** 1, pp.156-163 (2012)
32. P.K. Kadiyala, H. Chattopadhyay, Heat Transfer Engineering, doi: 10.1080/01457632.2017.1288045, pp. 1-9 (2017)
33. P. Ocłoń, S. Łopata, M. Nowak, A.C. Benim, Progress in Computational Fluid Dynamics, **15,** 5, pp.290-306 (2015)
34. S. Bhattacharyya, H. Chattopadhyay, A.C. Benim, Progress in Computational Fluid Dynamics, **17,** 3, pp. 193-197 (2017)
35. S. Bhattacharyya, H. Chattopadhyay, A. Swami, Md. K. Uddin, Int. J. Heat and Technology, **34,** 4, pp.727-733 (2016)
36. Z.Y. Guo, W.Q. Tao, R.K. Shah, International Journal of Heat Mass Transfer, **48**, pp.1797-1807 (2005)
37. S. Bhattacharyya, H. Chattopadhyay, A. Guin, A.C. Benim, Heat Tran. Eng., doi: 10.1080/01457632.2018.1474593 (2018)
38. S. Bhattacharyya, H. Chattopadhyay, A.C. Benim, Progress in Computational Fluid Dynamics, **17,** 6, pp. 390-396 (2017)